Constant-Intensity Waves in Non-Hermitian Media

Konstantinos G. Makris, Andre Brandstötter, and Stefan Rotter

Abstract When waves propagate through a non-uniform potential landscape their interference typically gives rise to a complex intensity pattern. In this chapter we review our work on how to entirely suppress these intensity variations by adding system-specific gain and loss components to the potential. The resulting constant-intensity (CI) waves are entirely free of interference fringes and get perfectly transmitted across any such non-Hermitian scattering landscape that is put in their way. We discuss how to generalize this concept to more than one dimension and to the non-linear regime where these special wave states open up the way to study the phenomenon of modulation instability in non-uniform potentials. Experimental implementations of these unique wave states are envisioned not just in optics, but also in other fields of wave physics such as in acoustics.

1 Introduction

Waves play an important role in many fields of science and in all of them the plane wave solution is the one that solves the corresponding wave equation in the most straightforward way. When placing a spatially varying potential in the way of such a plane wave, however, the problem becomes immediately less trivial as potentials typically reflect and scatter the wave, leading to interference and a non-uniform wave intensity that is strongly position-dependent. Such a potential could be an electrostatic field for an electronic matter wave, a non-uniform distribution of a dielectric medium for an electromagnetic wave or a wall that reflects an acoustic pressure wave. All of these cases lead to diffraction and wave interference,

K. G. Makris (✉)
Department of Physics, University of Crete, Heraklion, Greece
e-mail: makris@physics.uoc.gr

A. Brandstötter · S. Rotter
Institute for Theoretical Physics, Vienna University of Technology (TU Wien), Vienna, Austria
e-mail: andre.brandstoetter@tuwien.ac.at; stefan.rotter@tuwien.ac.at

D. Christodoulides, J. Yang (eds.), *Parity-time Symmetry and Its Applications*, Springer Tracts in Modern Physics 280,
https://doi.org/10.1007/978-981-13-1247-2_19

resulting in the highly complex variation of a wave's spatial profile that we are all very familiar with. Engineering these effects at one's will is a challenging task – think here, e.g., of the search for a cloaking device [1] or of the entire field of adaptive optics [2]. New strategies in this direction are thus in high demand and could establish a fertile ground in many of the different disciplines of science and technology in which wave propagation is a key element.

The starting point for our endeavor is the insight, that very unconventional phenomena arise in the situation where waves propagate and diffract in a suitably chosen spatial refractive index distribution that combines both gain and loss [3]. Such non-Hermitian potential regions [4, 5], which serve as sources and sinks for waves, respectively, can give rise to novel wave effects that are impossible to realize with conventional, Hermitian potentials. Examples of this kind, that were meanwhile also realized experimentally [6–10], are the uni-directional invisibility of a gain-loss potential [11], devices that can simultaneously act as a laser and as a perfect absorber [12–14] and resonant structures with unusual features like non-reciprocal light transmission [10] or loss-induced lasing [15–17]. In particular, systems with a $\mathscr{P}\mathscr{T}$-symmetry [18], where gain and loss are carefully balanced, have recently attracted enormous interest [19–24]. All these activities that were initially driven by the introduction of the counter-intuitive concept of $\mathscr{P}\mathscr{T}$-symmetry [18] in the realm of waveguide optics theoretically [19, 20] and experimentally [6, 7], opened a new area of research, that of non-Hermitian photonics or parity-time symmetric optics.

In the research presented below we extend the above concepts in a significant way. Specifically, we show here that for a general class of potentials that spatially combine gain and loss, it is possible to eliminate the intensity variations in wave scattering entirely, and create constant-intensity waves [25–28]. In particular, we present new solutions for a whole class of waves that have constant intensity even in the presence of a very irregular potential landscape. Quite surprisingly, these waves are solutions to both the paraxial equation of diffraction, the discrete and continuous non-linear Schrödinger equation, and the scalar Helmholtz scattering wave equation. In the linear regime, such constant-intensity waves resemble Bessel beams in free space [29] in that they carry infinite energy and propagate without distortion (depending on the truncation). In the non-linear regime, they provide the only background where the best known symmetry breaking instability, the so-called modulational instability (MI) [30–35] can be analyzed for the first time in inhomogeneous non-Hermitian potentials. Using these solutions for studying the phenomenon of MI, we find that, in the self-defocusing case, unstable finite size and periodic modes appear and cause the wave to disintegrate and to generate a train of complex solitons.

This book chapter follows in part our previously published manuscripts on the above subjects – see, in particular, the following three references [25, 26, 28] where also more details can be found.

2 Constant-Intensity Waves and Modulation Instability in Inhomogeneous Continuous Media

Following [25], we start from the well known non-linear Schrödinger equation (NLSE). This scalar wave equation encompasses both the physics of matter waves as well as many aspects of optical wave propagation. Specifically, we will consider the NLSE with a general, non-Hermitian potential $V(x)$ and a Kerr non-linearity,

$$i\,\partial_z \psi + \partial_x^2 \psi + V(x)\psi + \sigma|\psi|^2\psi = 0\,. \tag{1}$$

The scalar, complex valued function $\psi(x, z)$ describes the wave function of a matter wave as it evolves in time or the electric field envelope along a scaled propagation distance z. The non-linearity can either be self-focusing or de-focusing, depending on the sign of σ. For this general setting, we now introduce a whole family of potentials $V(x)$ which are determined by the following simple relation,

$$V(x) = W^2(x) + i\frac{dW(x)}{dx}, \tag{2}$$

where $W(x)$ is a given real generating function to which no further constraints apply (apart from smoothness). In the special case where $W(x)$ is an even function of x, the actual optical potential $V(x)$ turns out to be $\mathscr{P}\mathscr{T}$-symmetric, since $V(x) = V^*(-x)$. We emphasize, however, that our analysis is valid for all confined or periodic functions $W(x)$, which do not necessarily lead to a $\mathscr{P}\mathscr{T}$-symmetric form of $V(x)$. Rather, we can prove for the entire non-Hermitian family of potentials that are determined by Eq. (2), that the following analytical and stationary constant-intensity wave is a solution to the NLSE in Eq. (1),

$$\psi(x, z) = Ae^{i\sigma A^2 z + i\int W(x)dx}, \tag{3}$$

with a notably constant and real amplitude A. We emphasize here the surprising fact, that this family of solutions exists in the linear regime ($\sigma = 0$) as well as for arbitrary strength of non-linearity ($\sigma = \pm 1$). An interesting point to observe is that the above solutions exist only for non-Hermitian potentials, since for $W(x) \to 0$ we also have $V(x) \to 0$. Therefore, these families of counterintuitive solutions are the direct outcome of the non-Hermitian nature of the involved potential $V(x)$ and as such exist only for these complex structures.

In order to better understand and highlight the properties of such constant-intensity solutions we consider one-dimensional potentials that are generated by Hermite polynomials choosing $W(x) = H_n(x)e^{-Bx^2}$. The results for vanishing non-linearity ($\sigma = 0$) are illustrated in Fig. 1. Here, the localized optical potential $V(x)$ is not $\mathscr{P}\mathscr{T}$-symmetric (see Fig. 1a) and corresponds physically to a waveguide-coupler with lossy arms and optical gain in the evanescent region. If the initial beam is not designed to have the correct phase (as given by Eq. (3)), then the light diffracts

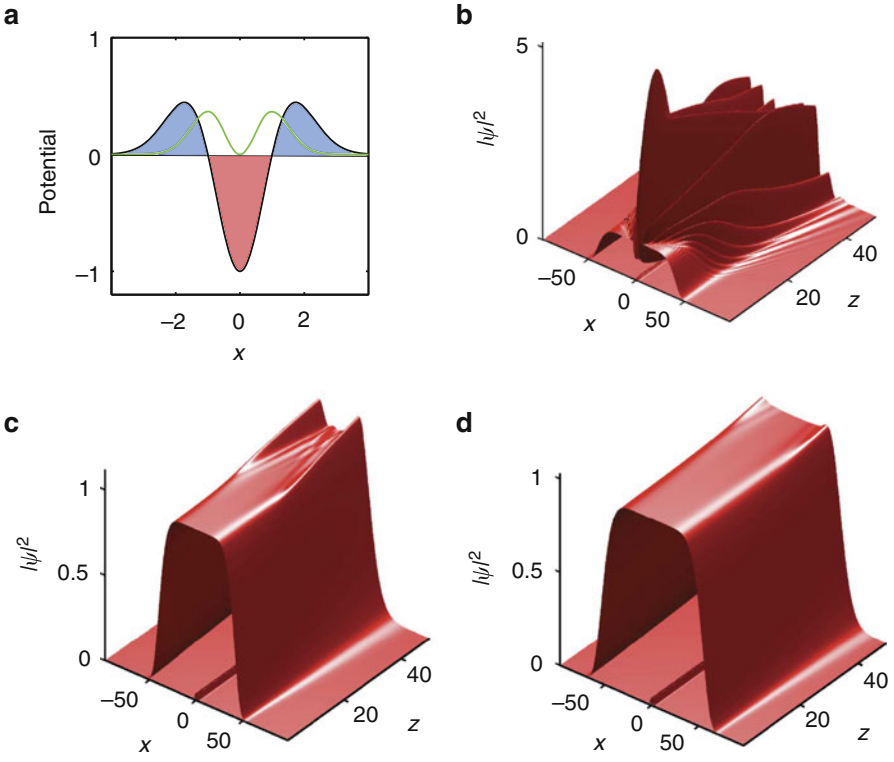

Fig. 1 (**a**) Real part (green line) and imaginary part (black line) of the complex potential $V(x)$ satisfying Eq. (2) (blue filled regions depict loss, whereas the red one depicts gain). (**b**) Evolution of a constant amplitude without the correct phase at the input at $z = 0$. (**c**, **d**) Spatial diffraction of the truncated constant-intensity solution satisfying the correct phase relation of Eq. (3). Two different input truncations are shown for comparison. The lines in the $x - z$ planes of (**b**, **c**, **d**) around $x = 0$ depict the real refractive index of the potential as shown in (**a**). Note the different vertical axis scale in (**b**)

fast to the gain region as we can see in Fig. 1b. The effects of truncation of the constant-intensity solution are shown in Figs. 1c, d. Similar to the diffraction-free beams [29], we find that the wider the width of the truncation aperture is, the larger is the propagation distance after which the beam starts to diffract. In the case of no truncation (i.e., infinitely wide aperture) diffraction is fully suppressed for an infinitely long propagation distance.

In a next step we demonstrate that the above concepts are not restricted to a single spatial dimension x (apart from the propagation distance z), but can easily be generalized to two spatial dimensions x, y. The family of these complex potentials $V(x, y)$ and the corresponding constant-intensity solutions $\psi(x, y, z)$ of the two-dimensional NLSE $i\frac{\partial\psi}{\partial z} + \frac{\partial^2\psi}{\partial x^2} + \frac{\partial^2\psi}{\partial y^2} + V(x, y)\psi + \sigma|\psi|^2\psi = 0$ are given as follows:

$$V(x, y) = |\mathbf{W}|^2 - i\nabla \cdot \mathbf{W}\,, \tag{4}$$

$$\nabla \times \mathbf{W} = 0\,, \tag{5}$$

$$\psi(x, y, z) = Ae^{i\sigma A^2 z + i\int_C \mathbf{W} d\mathbf{x}}\,, \tag{6}$$

where $\mathbf{W} = \mathbf{x}W_x + \mathbf{y}W_y$ with W_x, W_y being real functions of x, y and C being any smooth open curve connecting an arbitrary point (a, b) to any different point (x, y). As in the one-dimensional case, these solutions are valid in both linear and non-linear domains. For the particular case of $W_x = \cos(x)\sin(y)$, $W_y = \cos(y)\sin(x)$, the resulting periodic potential $V(x, y)$ is that of an optical lattice with alternating gain and loss waveguides. The imaginary part of such a lattice is illustrated in Fig. 2a. In Fig. 2b, we display the diffraction of a constant-intensity beam with the correct phase (as in Eq. (6)) launched onto such a linear lattice ($\sigma = 0$) through a circular aperture. As we can see, the beam maintains its constant intensity over a remarkably long distance. The transverse Poynting vector defined as $\mathbf{S} = (i/2)(\psi\nabla\psi^* - \psi^*\nabla\psi)$, is presented in Fig. 2c and the light always flows following complicated stream line patterns from the gain regions to the loss regions in a symmetric fashion. Once the finite beam starts to diffract this balanced flow is disturbed and all the light is concentrated only in the gain regions.

These unique diffraction-free and constant-intensity waves are also solutions of the NLSE for both the self-focusing and defocusing cases. As a result, we can study now for the first time their modulation instability under small perturbations. In other words, we want to investigate how perturbations of the exact CI solutions get reinforced by the non-linearity leading to a break up of the waveform into a complex pattern. Specifically, we are interested in understanding the linear stability of the solutions of Eq. (1) of the form $\psi(x, z) = [A + \varepsilon F_\lambda(x)e^{i\lambda z} + \varepsilon G^*_\lambda(x)e^{-i\lambda^* z}]e^{i\theta(x,z)}$, where the phase function is $\theta(x, z) = \sigma A^2 z + \int W(x)dx$. Here, $F_\lambda(x)$ and $G_\lambda(x)$ are the perturbation eigenfunctions with $\varepsilon \ll 1$ and the imaginary part of λ measures the instability growth rate of the perturbation. To leading order in ε, we obtain the following linear eigenvalue problem for the two-component perturbation eigenmodes $\boldsymbol{\varphi_\lambda}(x) \equiv [F_\lambda(x)G_\lambda(x)]^T$, the eigenvalues of which are λ, i.e., $\overleftrightarrow{M}(\hat{L}_\pm)\cdot\boldsymbol{\varphi_\lambda}(x) = \lambda\boldsymbol{\varphi_\lambda}(x)$. The operator matrix $\overleftrightarrow{M}$ is defined by the following expression:

$$\overleftrightarrow{M}(\hat{L}_\pm) = \begin{pmatrix} \hat{L}_+ & \sigma A^2 \\ -\sigma A^2 & -\hat{L}_- \end{pmatrix}. \tag{7}$$

Here the appearing linear operators are defined by the following relationships:

$$\hat{L}_\pm = \hat{L}_0 \pm i\hat{L}_1 \tag{8}$$

$$\hat{L}_0 = \sigma A^2 + d^2/dx^2 \tag{9}$$

$$\hat{L}_1 = 2W(x)d/dx \tag{10}$$

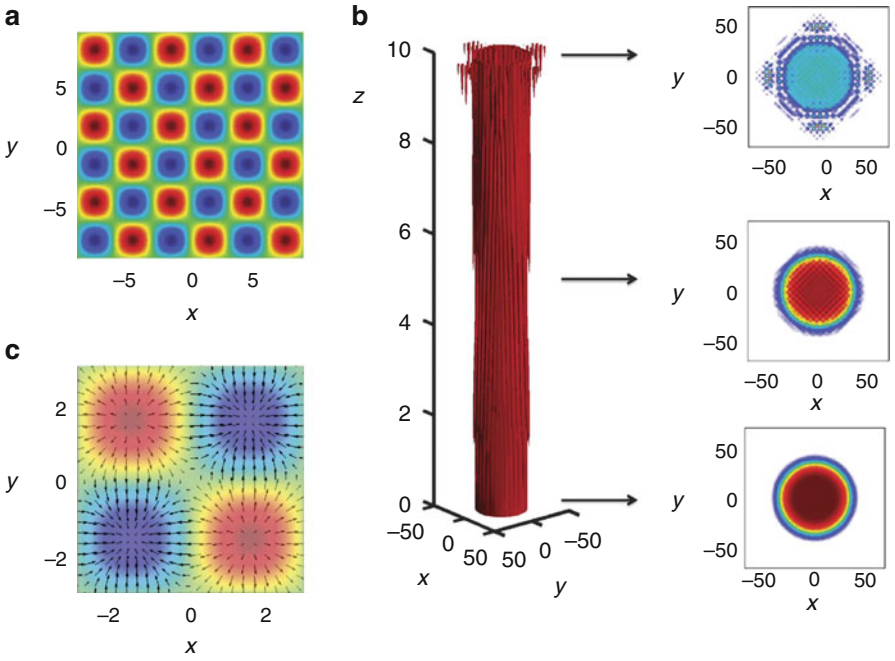

Fig. 2 Imaginary part of the complex potential $V(x, y)$ discussed in the text. Red and blue regions correspond to gain and loss, respectively. (**b**) Iso-contour of the beam intensity launched onto the potential in (**a**) through a circular aperture of radius $\sim 40\lambda_0$, where λ_0 is the free space wavelength. Also shown are three transverse intensity plots (from bottom to top) at $z = 0$, $z = 5$, $z = 10$. (**c**) Transverse power flow pattern (indicated by arrows) of the beam at $z = 5$

So far the above discussion is general and applies to any smooth function W (periodic or not) that is real. The eigenspectrum analysis of the above eigenvalue problem determines whether the constant-intensity solution is stable ($\lambda \in \mathbb{R}$) or unstable ($\lambda \in \mathbb{C}$). We now apply this analysis to study the modulation instability of constant-intensity waves in $\mathscr{P}\mathscr{T}$-symmetric optical lattices [19, 20] assuming that $W(x)$ is a periodic potential with period α. In particular, we consider the example of a $\mathscr{P}\mathscr{T}$-symmetric photonic lattice where $W(x) = \frac{V_0}{2} + V_1 \cos(x)$ and the resulting optical potential is $V(x) = [\frac{V_0^2}{4} + V_1^2 \cos^2(x) + V_0 V_1 \cos(x)] + i V_1 \sin(x)$. The corresponding constant-intensity solution, whose modulation instability we want to study is given by $\psi(x, z) = A \exp[i\sigma A^2 z + i\frac{V_0 x}{2} + i V_1 \sin(x)]$. In order for this constant-intensity solution to be periodic in x with the same period as the lattice, the constant term V_0 must be quantized, namely $V_0 = 0, \pm 2, \pm 4, \ldots$. For all the subsequent results we will always assume that $V_0 = 4$ and $V_1 = 0.2$ (without loss of generality). It is important to note here, that for our $\mathscr{P}\mathscr{T}$-lattice V(x) is in the so-called 'unbroken $\mathscr{P}\mathscr{T}$-symmetric phase' with only real propagation constants.

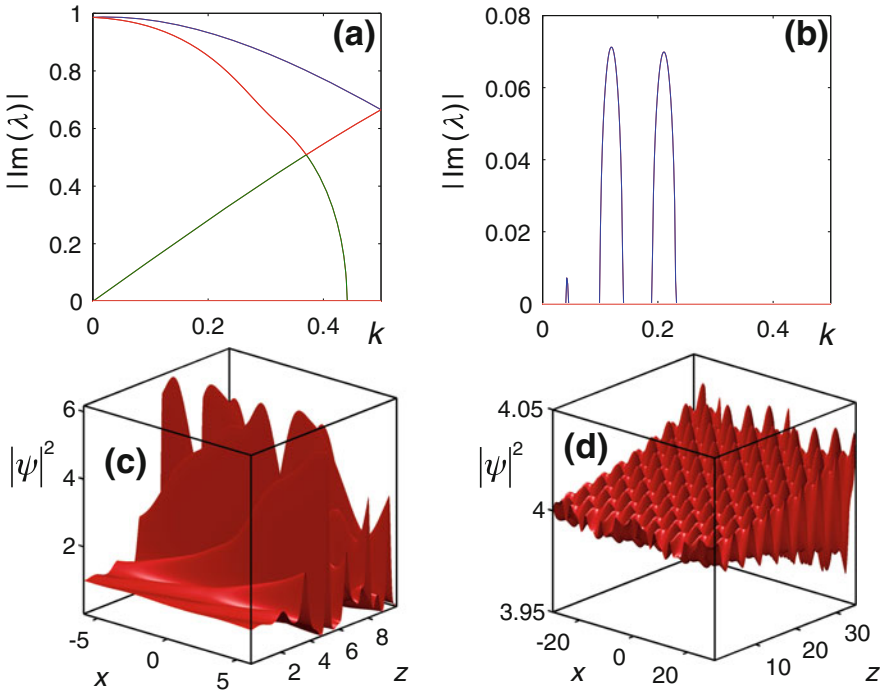

Fig. 3 (**a**, **b**) Modulation instability growth rate as a function of the Bloch momentum (half of first Brillouin zone), for (**a**) self-focusing non-linearity ($\sigma = 1$) and amplitude $A = 1$, and for (**b**) defocusing non-linearity ($\sigma = -1$) and amplitude $A = 2$. Different colors in (**a**), (**b**) denote different instability bands. (**c**, **d**) Numerical results for the intensity evolution of a constant-intensity wave for (**c**) a self-focusing non-linearity with parameters $k = 0$, $A = 1$, $\varepsilon = 0.01$, and (**d**) for a defocusing non-linearity with parameters $k = 0.22$, $A = 2$, $\varepsilon = 0.001$. The peak values are indicated on the vertical axes and match very well with the results of our perturbation analysis

In the broken phase some of these eigenvalues are complex and the instabilities are physically expected. Since $W(x)$ is periodic we can expand the perturbation eigenvectors $\boldsymbol{\varphi_\lambda(x)}$ in a Fourier series and construct numerically the bandstructure of the stability problem. So at this point we have to distinguish between the physical band-structure of the problem and the perturbation band-structure of the stability problem. Based on the above, the Floquet-Bloch theorem implies that the eigenfunctions $\boldsymbol{\varphi_\lambda(x)}$ can be written in the form $\boldsymbol{\phi_\lambda(x)} = \phi(x,k)e^{ikx}$, where $\phi(x,k) = \phi(x+\alpha,k)$ with k being the Bloch momentum of the stability problem. The results are illustrated in the following Fig. 3a for a self-focusing non-linearity ($\sigma = 1$) and for the amplitude $A = 1$. More specifically, we show the instability growth rate $|\mathrm{Im}\{\lambda(k)\}|$ as a function of the perturbation eigenvector k in the first half Brillouin zone, and we can see that the constant-intensity waves are linearly unstable for any value of Bloch momenta of the imposed perturbation.

The situation is different for the defocusing case ($\sigma = -1$) where the results are presented in Fig. 3b. For some values of k the constant-intensity solutions are linearly stable and their instability dependence forms bands reminiscent of the bands appearing in conventional MI results for bulk or periodic potentials [30, 33, 34], but quite different and profoundly more complex. In order to understand the physical outcome of such instabilities and how they lead to filament formation, we have performed direct numerical simulations for the dynamics of the constant-intensity solutions against specific perturbations. The results are presented in Fig. 3c, d. More specifically, we examine the intensity evolution of a constant-intensity solution when it is perturbed by a specific Floquet-Bloch mode. In other words, at the input of the lattice at $z = 0$, we have $\psi(x, z = 0) = [A + \varepsilon F_\lambda(x) + \varepsilon G^*_\lambda(x)]e^{i\theta(x,0)}$, and we are interested to see if the linear stability analysis captures the exponential growth of the imposed perturbations. For the considered $\mathscr{P}\mathscr{T}$-lattice with self-focusing non-linearity, we examine the non-linear dynamics of the constant-intensity solution and the result is presented in Fig. 3c. For a perturbation eigenmode with Bloch momentum $k = 0$ and $A = 1$, $\varepsilon = 0.01$, we can see from Fig. 3a that $\mathrm{Im}\{\lambda(0)\} \sim 1$. Therefore, we can estimate the growth for a propagation distance of $z = 5$ to be around $|1+0.01\cdot e^{1\cdot 5}|^2 \sim 6.1$, which agrees very well with the dynamical simulation of Fig. 3c. Similarly, for the defocusing non-linearity, and for parameters $k = 0.22$ and $A = 2$, $\varepsilon = 0.001$, we estimate the growth for a propagation distance $z = 35$ to be around $|2+0.001\cdot e^{0.046\cdot 35|^2} \sim 4.02$, which matches exactly with the propagation dynamics result of Fig. 3d.

We would like to mention here that the above MI analysis can be extended to vectorial non-linear Schrödinger equations for which multi-component constant intensity solutions exist [27].

3 CI-Waves in Discrete Disordered Lattices

Engineering a continuous distribution of gain and loss that perfectly matches the requirements of our theoretical analysis is a challenging task experimentally. To facilitate an experimental implementation, we thus also study whether our concepts can be applied to discrete rather than to continuous potential landscapes (see Fig. 4a,b for an illustration of these two cases). Consider, for this purpose, a lattice of coupled non-Hermitian single-mode waveguides as depicted in Fig. 4a extending along the positive z-direction. The propagation of light in such a lattice can be described using coupled mode theory. Specifically, the beam evolution is governed by the following normalized paraxial equation of diffraction for N coupled optical elements (waveguides or cavities),

$$i\frac{dU_n}{dz} + c(U_{n+1} + U_{n-1}) + (\beta_n + ig\gamma_n)U_n = 0\,, \tag{11}$$

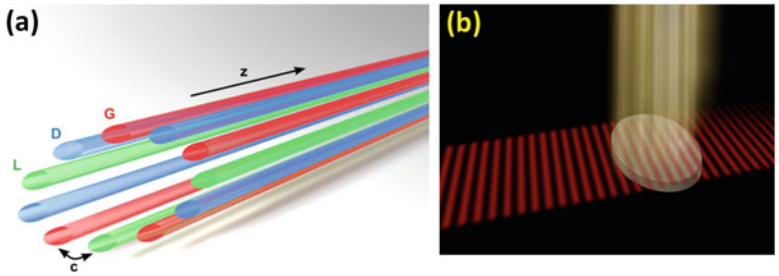

Fig. 4 (**a**) Schematics of a non-Hermitian lattice of coupled optical waveguides, that supports constant-intensity modes. The waveguides form a ring, corresponding to periodic boundary conditions. The labels D, L, G, c stand for a dielectric, loss, gain element, and for the coupling constant, respectively. (**b**) One of the envisioned goals to realize constant-intensity waves: by shining light through a spatial light modulator from the top, one can non-uniformly pump the gain medium inside a material to obtain a spatially varying gain-loss profile that makes the medium invisible for an incident wave from one side

where $U_n(z)$ represents the amplitude of the electric field envelope, z is the propagation distance, c is the coupling between adjacent neighbors (here taken to be equal to one, without any loss of generality) and $n = 1, \ldots N$ the waveguide index. Each channel is characterized by either gain ($\gamma_n < 0$) or loss ($\gamma_n > 0$) and by its real refractive index β_n. The gain-loss amplitude is described by the parameter g. For $g = 0$ the system is obviously Hermitian. The main question we will address for the case of an optical non-Hermitian lattice is if and under which conditions constant-intensity waves exist [26]. Specifically, we are looking for stationary constant-intensity solutions of the form:

$$U_n(z) = e^{i\theta_n} e^{i\lambda z}\,, \tag{12}$$

where θ_n is a given phase distribution over all waveguide channels and λ is the propagation eigenvalue. It is important to understand that in order for such CI-modes to exist, periodic boundary conditions must be imposed at the end points of the lattice. In particular, the Born-Von Karman periodic boundary conditions must be valid for the field, namely:

$$U_0 = U_N, U_{N+1} = U_1\,. \tag{13}$$

We can see that the complex refractive index must satisfy (for any given phase distribution):

$$\beta_n = \lambda - \cos(\theta_{n+1} - \theta_n) - \cos(\theta_{n-1} - \theta_n)\,, \tag{14}$$

$$\gamma_n = -\sin(\theta_{n+1} - \theta_n) - \sin(\theta_{n-1} - \theta_n)\,. \tag{15}$$

Since the constant-intensity wave of Eq. (12) must satisfy the periodic boundary conditions, it is also true that the phase distribution must satisfy the relations:

$$\theta_0 = \theta_N, \theta_{N+1} = \theta_1 . \tag{16}$$

Physically speaking, the periodic boundary conditions correspond to an optical ring-lattice of coupled optical elements (waveguides or cavities), as schematically depicted in Fig. 4a. The given phase distribution θ_n determines the real and imaginary parts of the refractive index (through Eqs. (14) and (15)) and the eigenvalue λ (which can be removed by a gauge transformation) affects only the real part of the index of refraction. An important difference between the solutions found in the continuum case studied in the previous chapter and those found here is the following: The CI-waves in the continuous and infinite case are radiation eigenmodes, while in the discrete and periodic problem at hand they are true eigenmodes (more precisely supermodes) of the entire system. We have also to note that for $\lambda = 0$, the CI-mode is unidirectionally invisible, since the wave propagates without any additional phase change and only in one propagation direction (for the opposite direction the complex conjugate potential must be used).

We have thus found that for system configurations satisfying Eq. (11) the complex refractive index can always be engineered to yield a CI solution. This is particularly remarkable in view of the fact that disordered waveguide lattices without any gain and loss give rise to Anderson localization – a well-studied phenomenon in condensed matter physics [36–40]. The existence and properties of localized modes in linear random systems has meanwhile been thoroughly investigated. The majority of the theoretical and experimental studies have, however, been concentrated on Hermitian media (with the exception of the random laser literature) where Anderson localization is now well understood. Adding gain and loss to the medium makes the fundamental question of localization generally more complicated [41]. In this context our results now provide the interesting insight that any disordered medium that gives rise to Anderson localization (without gain and loss) can also produce extended modes of uniform intensity (CI-supermodes) when a suitable combination of gain and loss is added.

In Fig. 5 such a random system of 100 coupled waveguides is considered. The real and imaginary part of the refractive index distribution is depicted for a particular realization of the lattice in Fig. 5a, b, respectively. As we can see, adding gain and loss to such a system alters the Anderson localized modes of the Hermitian lattice to extended delocalized modes, one of which is a CI-supermode (Fig. 5c) with a real eigenvalue (Fig. 5d).

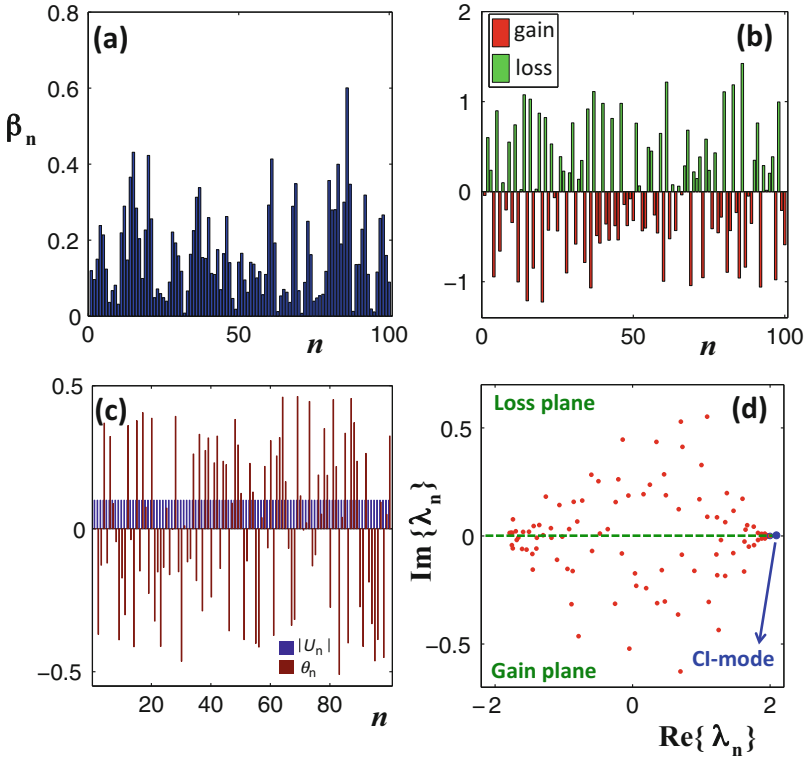

Fig. 5 CI-mode (with $\lambda = 2$, $g = 1$) in a disordered lattice of $N = 100$ waveguides with a random phase. In particular, (**a**) real part and imaginary parts of the refractive index per waveguide, (**b**) gain and loss per channel, (**c**) the amplitude and phase of the CI-supermode, and (**d**) eigenvalue spectrum in the complex plane. The eigenvalue of the CI-supermode is denoted with a blue circle

4 CI-Waves in the Scattering Regime

In all of the above considerations, the variation of the refractive index or of the potential was considered only in the direction transverse to the propagation direction. The question we want to address in the following is, whether CI waves also exist for the case that the potential variation occurs in the direction along which a wave is propagating. In particular, it would be very exciting to see if we can create in this way a "scattering state" that perfectly penetrates a disordered medium with constant intensity. The scattering of waves through disordered media has, in fact,

captured the interest of various communities for quite some time now [42–44]. While much work has been invested into understanding the *statistical* properties of the corresponding wave transport [45] there has recently been a surge of interest in controlling the scattering of waves through *individual* systems for specific purposes such as detection, imaging, and efficient transmission across disordered materials [46, 47]. Remarkable progress in these endeavors has recently been made in the optical domain, largely due to the availability of spatial light modulators and new concepts for how to apply them on turbid media [48, 49]. In a first generation of corresponding experiments the focus was laid on shaping the input wave front impinging on an immutable disordered sample such as to achieve a desired output, like a spatial or temporal focus behind the medium [50–53]. More recent studies concentrated instead on controlling the medium itself, e.g., through the material fabrication process [54] or through a spatially modulated pumping [55], leading, e.g., to a versatile control of random and micro-cavity lasers [56–60].

Here we will build on these advances and shall combine them with our insights on how to construct CI waves [28]. Specifically, we show that for a general disordered medium, given by a distribution of the real part of the refractive index $n_R(x)$, a corresponding distribution of its imaginary part $n_I(x)$ can be found, such that a wave propagating through this continuous medium will feature a constant intensity throughout the entire non-uniform scattering landscape. In other words, we demonstrate that adding a judiciously chosen distribution of gain and loss to a disordered medium will make waves lose all their interference fringes including perfect transmission through the disorder.

The solution strategy that we explore for this purpose is based on the one-dimensional normalized Helmholtz equation that describes time-independent scattering of a linearly polarized electric field $\psi(x)$ both in forward and in backward direction,

$$\left[\partial_x^2 + \varepsilon(x)\, k^2\right] \psi(x) = 0\,. \tag{17}$$

Here $\varepsilon(x)$ is the dielectric function varying along the spatial coordinate x and $k = 2\pi/\lambda$ is the wavenumber (with λ being the wavelength). The dielectric function is complex thus $\varepsilon(x) = [n_R(x) + i n_I(x)]^2$, where $n_R(x)$, $n_I(x)$ denote the real and imaginary parts of the refractive index. In general, when a plane wave is incident on a spatially varying distribution $\varepsilon(x)$, interference takes place between the waves propagating forward and backward. As a result, a complex interference pattern is produced with fringes on its intensity. As we will now show, this fundamental physical picture can be quite different in the case of non-Hermitian media with loss and/or gain.

To jump right to the heart of the matter, we start with an ansatz for a constant-intensity (CI) wave with unit amplitude, $\psi(x) = \exp[iS(x)]$, where $S(x)$ is a real valued function. Due to the obvious relation to WKB-theory [61], we will derive the CI solution of the Helmholtz Eq. (17) in the bulk, by demanding that the ansatz $\psi(x) = \exp[iS(x)]$ has to be exact in the first order WKB-

approximation. Expanding the function $S(x)$ in powers of a small parameter δ, $S(x) = \frac{1}{\delta} \sum_{n=0}^{\infty} \delta^n S_n(x)$, and inserting it into the Helmholtz Eq. (17) to leading order, we can show that in the limit of $\delta \to 0$, δ scales with $1/k$. Setting $\delta = 1/k$ and collecting terms with the same power of k, we can write down the two dominant terms:

$$k^2 = \tfrac{1}{\delta^2} : \mathrm{Re}[\varepsilon(x)] + i\,\mathrm{Im}[\varepsilon(x)] - [S_0'(x)]^2 = 0 \tag{18}$$

$$k^1 = \tfrac{1}{\delta^1} : i\,S_0''(x) - 2\,S_0'(x)\,S_1'(x) = 0 \tag{19}$$

The exactness requirement of our ansatz necessitates that all terms $S_{n>0}$ are zero and the demand for constant intensity of $\psi(x)$ calls for a real-valued $S_0(x)$. Both conditions can be fulfilled by choosing $\mathrm{Im}[\varepsilon(x)] = -S_0''(x)/k$ such that the term $\mathrm{Im}[\varepsilon(x)]$ moves from Eqs. (18) to (19) leading to $\mathrm{Re}[\varepsilon(x)] = [S_0'(x)]^2$ and $S_1'(x) = 0$. As a result $S_1(x) = const.$ and all higher terms are constant as well. Setting $S_0'(x) = W(x)$, we finally obtain the non-Hermitian dielectric function (relative permittivity),

$$\varepsilon(x) = W^2(x) - \frac{i}{k}\,\partial_x W(x)\,, \tag{20}$$

with a corresponding CI solution $\psi(x) = \exp[ik \int W(x')dx']$ that is an exact solution of the Helmholtz equation and valid for the whole bulk space and all wavelengths. In other words, we identify a general class of refractive index distributions where real and imaginary parts are connected through the generating function $W(x)$, for which the fringes in the interference pattern vanish entirely. The fact that $W(x)$ can be chosen arbitrarily, with no limitations on its spatial complexity (apart from smoothness), is a key asset of this approach, making it very generally applicable. For the special case that the generating function is left-right symmetric, $W(x) = W(-x)$, the dielectric function is $\mathscr{P}\mathscr{T}$-symmetric since $\varepsilon(x) = \varepsilon^*(-x)$. Independently, however, of whether $\varepsilon(x)$ is $\mathscr{P}\mathscr{T}$-symmetric or not it can be shown that CI waves can also be found for all dielectric functions that are described by Eq. (20) in a finite domain $x \in [-D, D]$, bordering on free space for $x < -D$ and $x > D$. In this case, the scalar Helmholtz equation (17) admits the following exact CI wave solutions $\psi(x)$:

$$\exp[ik\,(x + D)], \quad x < -D\,, \tag{21}$$

$$\exp[ik \int_{-D}^{x} W(x')dx'], \; -D \le x \le D\,, \tag{22}$$

$$\exp[ik\,(x - D + c)], \quad x > D\,, \tag{23}$$

with c being a constant that is determined by the definite integral of W over the entire scattering region, in order for the field continuity relations to be satisfied.

Most importantly, the above solution does not only feature a constant intensity $|\psi(x)|^2 = 1$ in the asymptotic regions $x \leq -D$ and $x \geq D$, where $\varepsilon(x) = 1$ and simple plane wave propagation is realized, but also inside the finite region of length $2D$ in which the dielectric function varies and the phase-evolution is non-trivial. Regarding the appropriate boundary conditions at $x = \pm D$, it can be shown that the perfect transmission boundary conditions (zero reflection) [24] $\partial_x \psi(\pm D) = ik\psi(\pm D)$ imply the following conditions for the generating function, $W(\pm D) = 1$. From this result it is also clear that for vanishing imaginary part, the dielectric function, as defined in Eq. (20), reduces to $\varepsilon(x) = 1$, in which limit our CI wave solution is just a plane wave in free space.

It is also important to note that the wavenumber k appearing in the dielectric function $\varepsilon(x)$ of Eq. (20) is the same as the wavenumber k in the CI wave solution given in Eq. (21). In other words, for any value of k for which a CI scattering state is desired, the dielectric function $\varepsilon(x)$ has to be engineered correspondingly. Once $\varepsilon(x)$ is fixed and plane waves with varying values of k are impinging on this dielectric structure, a perfectly transmitting CI solution in general only occurs at the predetermined k value inherent in the design of $\varepsilon(x)$, whereby no issue arises with the Kramers-Kronig relations.

To elucidate the above ideas, we consider now one specific example of an index distribution and study the CI-waves it gives rise to. We assume $W(x)$ to be a parabolic function modulated with a cosine, namely $W(x) = [1 - 0.2\cos(15\pi x/2)](2 - x^2)$. The corresponding real part of the refractive index distribution $n_R(x)$ is shown as the gray shaded area in Fig. 6. A wave impinging on this dielectric structure composed of only $n_R(x)$ is partly reflected and features a highly oscillatory profile, see Fig. 6a. Quite in contrast, when adding also the gain and loss inherent in the imaginary index component $n_I(x)$ derived from $W(x)$ (see green and red regions in Fig. 6b), the resulting scattering state is fully

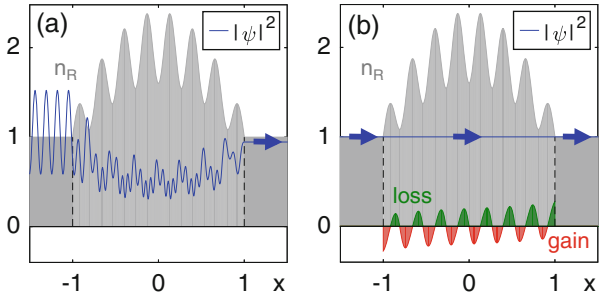

Fig. 6 (**a**) Scattering wave function intensity (blue line) in a Hermitian refractive index distribution for an incident plane wave (from the left) with a specific normalized wavenumber $k = 2\pi/0.26 = 24.15$. (**b**) Intensity of the CI-wave for the corresponding non-Hermitian refractive index $n(x)$ and the same incident plane wave. The real part of the refractive index is shown in gray, whereas its imaginary part is colored in green (loss) and red (gain). For illustration purposes the imaginary part in (**b**) was multiplied by a factor of 2. The calculations were performed using the transfer matrix approach

transmitted and features a constant intensity. Because of the boundary conditions, $W(x)$ must be symmetric at the end points of the cavity, resulting in an anti-symmetric distribution of $n_I(x)$. Our example shows that for a plane wave at an arbitrary incident wavenumber k, we can find the corresponding gain-loss landscape (from Eq. (20)), such that this wave will fully penetrate the scattering medium without forming any spatial variations in its intensity pattern.

Fixing a refractive index through Eq. (20) that leads to a CI wave at the specific wavenumber k_0, one can ask the question what happens to incident plane waves with detuned wavenumbers $k \neq k_0$. Naively, one may expect that the emergence of CI waves is a sharp resonance phenomenon, so that waves with a slight detuning in the wavenumber k should show a completely different behavior as, e.g., around a resonance in a Fabry-Perot interferometer [62]. This picture turns out to be misleading on several levels: Since the CI wave function at position x, $\psi(x) = \exp[ik\int_{-D}^{x} W(x')dx']$, only depends on the generating function $W(x')$ evaluated at values $x' < x$, one can easily truncate the system at any point x and still get a CI wave – provided one continues the system for all $x' > x$ with a constant generating function that has the same value as at the point of truncation. This behavior indicates that a refractive index profile that supports CI waves is not only reflectionless in total, but also unidirectional at any point inside a given structure. Perfect transmission in such systems is thus not a resonance phenomenon, suggesting that CI waves are stable against changes of the incident wavelength. To check this explicitly, we numerically calculated the average resonance width of the transmission spectrum $|t(k)|$ of the Hermitian system in Fig. 6, $\langle \Delta k_{Herm} \rangle = 0.84$, in an interval $k \in [\frac{2\pi}{0.5} - 3, \frac{2\pi}{0.5} + 3]$, with minimum transmission $|t(k)_{min}| = 0.77$. The transmission of the corresponding CI system (that of Fig. 6 but for the slighlty different wavenumber $k_0 = \frac{2\pi}{0.5}$) stays larger than 0.9 over the entire k-interval (not shown), confirming our prediction.

Another important point to make is that one can easily achieve a transmission equal to one in a non-Hermitian system just by adding enough gain to it. In a CI system, however, the net average amplification is zero, since $\int_{-D}^{D} \mathrm{Im}[\varepsilon(x)]dx = 0$ and the intensity is equally distributed everywhere. Additionally, the material gain corresponding to the potentials examined for $\lambda = 1.5\,\mu\mathrm{m}$ is around a realistic value of $80\,\mathrm{cm}^{-1}$ for $\max(n_I) = 10^{-3}$. Moreover, these uniform intensity waves are still valid for any slowly varying or rapidly fluctuating (subwavelength) optical potential (as exact solutions of Helmholtz equation). For these reasons the aforementioned physical values depend on the size of the scattering region, and on the operation wavelength.

The most striking application of CI waves occurs for the case of scattering through disordered environments. From the discussion above on the disordered lattices we already know that in strongly scattering disordered media Anderson localization occurs. For scattering states like the ones considered here, Anderson localization results in an exponential decrease of the transmittance $T = |t|^2$ for structures with sizes greater than the localization length $\xi = -2D\langle \ln[T(D)] \rangle^{-1}$. For a given real and disordered index of refraction in the localized regime close

to unit transmittance is thus very unlikely and occurs only at well-isolated, sharply resonant wave numbers that are difficult to achieve experimentally [63, 64]. Our approach now allows to turn this behavior upside down – not only in the sense that we can engineer unit transmission at any predetermined value of the wavenumber k, but also that we can create scattering states that have constant intensity in a strongly disordered environment which would usually give rise to the most dramatic intensity fluctuations known in wave physics.

We illustrate our results for the disordered one-dimensional slab shown in Fig. 7, where a refractive index distribution following Eq. (20) is considered with a tunable imaginary component, $\varepsilon(x) = [n_R(x) + i\,a\,n_I(x)]^2$ (the tunable parameter a controls the overall amplitude of gain and loss). More specifically, the generating function $W(x)$ is a superposition of 99000 Gaussian functions of the same amplitude and width, but centered around random positions. For $a = 0$ the refractive index is Hermitian, whereas for $a = 1$ CI waves exist. The refractive index distribution of such a non-Hermitian disordered medium is depicted in Fig. 7a, and the localization length ξ of the Hermitian refractive index ($a = 0$) is depicted in Fig. 7b. Without the gain and loss distribution, the system reflects almost all waves due to localization. Adding first only the gain part of the CI refractive index distribution (see Fig. 7c) still results in highly oscillatory scattering wave functions with finite reflectance for all values of the gain amplitude a (from 0 to 1), see Fig. 7d. Quite counterintuitively, adding also the loss part of the CI index distribution leads to perfect and fringe-free transmission for $a = 1$, see Fig. 7e. By varying the gain-loss amplitude a, as in Fig. 7e, we can also see the smooth transition from the Anderson localization regime (at $a = 0$) to perfect transmission with constant intensity (at $a = 1$).

Another important aspect of CI waves is their experimental realization, with the most challenging part being the fabrication of a specific index distribution with gain and loss [65]. In order to overcome such inherent difficulties, we study here also the existence of CI scattering states in a system of discrete elements, see Fig. 8. Such a set-up is composed of many discrete sites (cavities) with gain or loss and a specific real refractive index distribution. Translating the analytic solution of Eq. (20) to a finite-difference model, yields the following discrete solution that satisfies the discrete version of the Helmholtz equation with the discrete dielectric elements ε_m and the CI scattering state ψ_m:

$$\varepsilon_m = b^{-2}\left\{2 - e^{\frac{ik\Delta x}{2}(W_m+W_{m+1})} - e^{-\frac{ik\Delta x}{2}(W_m+W_{m-1})}\right\} \tag{24}$$

and

$$\psi_m = \exp\left[\frac{ik\Delta x}{2}\left(W_1 + W_m + 2\sum_{n=2}^{m-1} W_n\right)\right], \tag{25}$$

where $b = \omega\Delta x$, $\omega^2 = 2\,[1-\cos(k\Delta x)]/\Delta x^2$, and $m = 1, \ldots, M$. Additionally, perfect transmission boundary conditions imposed at the endpoints of the discrete chain of the scatterers $\psi_0 = \psi_1 \exp(-ik\Delta x)$, and $\psi_{M+1} = \psi_M \exp(ik\Delta x)$ as

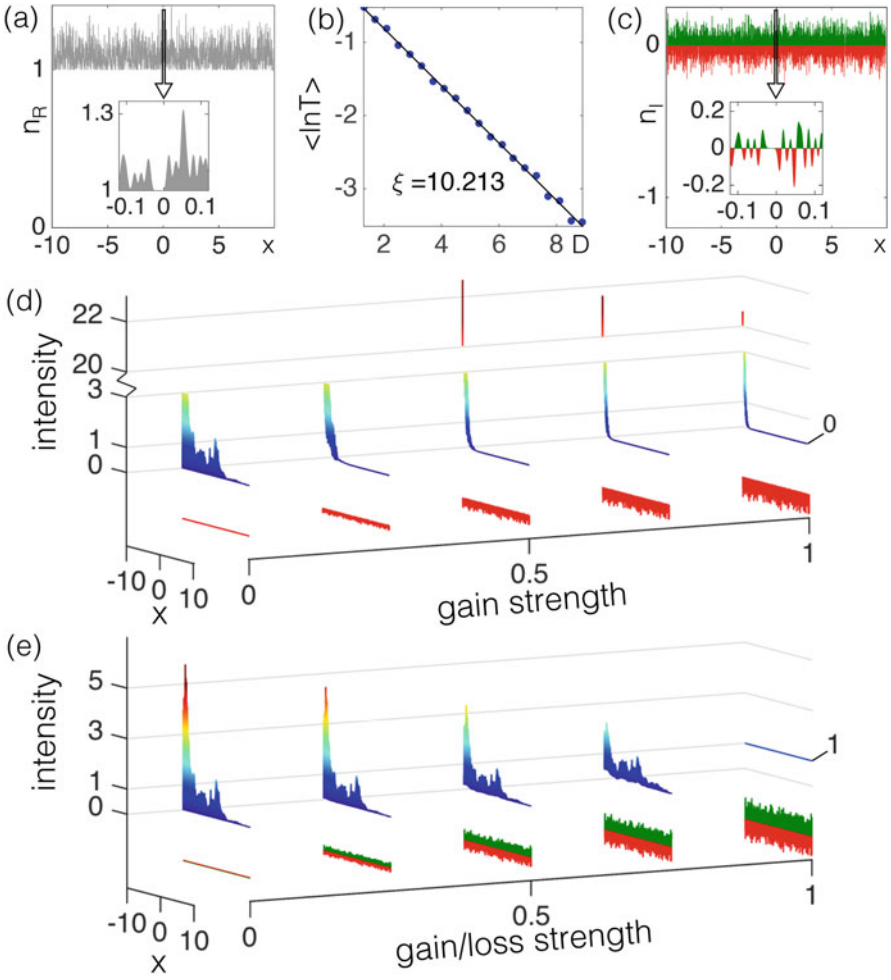

Fig. 7 A strongly disordered potential consisting of $N = 99000$ Gaussian scatterers is considered. (**a**) The corresponding refractive index distribution $n_R(x)$ in a small interval of x is shown. (**b**) Exponential suppression of the transmittance T with localization length ξ in this system for variable length of the disordered region D. (**c**) Imaginary part of the refractive index $n_I(x)$ following from the CI design principle ($n_I(x)$ is matched to the real index distribution in (**a**)). (**d**, **e**) Scattering wave functions for the disordered region as a function of the gain-loss strength parameter a, for the gain-only and gain-loss potential, respectively. In both cases, an incident plane wave is considered (from left to right). The CI-wave can be clearly seen for the full gain-loss strength ($a = 1$) in (**e**)

well as the relation $\omega \Delta x < 2$ must always hold. We consider a specific example in Fig. 8 of M-elements that form a one-dimensional disordered chain. By adding gain or loss onto the sites as prescribed by Eq. (24), an incoming wave from the left will have the same constant intensity on all of these sites.

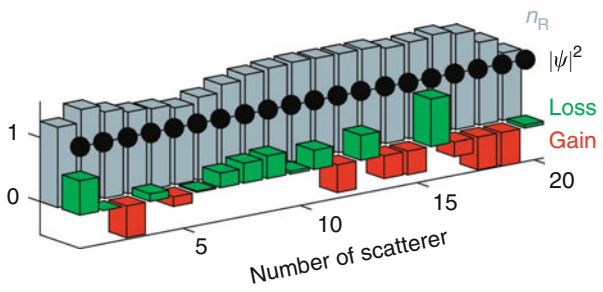

Fig. 8 Disordered chain of discrete scatterers with an incoming plane wave from the left. The real part (gray) as well as the gain (red) and loss (green) components of the refractive index are shown for each scatterer. The corresponding discrete CI-wave is depicted with black dots. The normalized parameters used are $M = 20$, $\omega = 12$, $L = 2$ and $\Delta x = L/(M - 1)$

5 Future Directions and Outlook

In conclusion, we have presented an overview of recent results related to constant-intensity waves in non-Hermitian systems such as synthetic media with gain and loss. The central idea of this line of research is to spatially engineer the imaginary part of the index of refraction in order to obtain a desired field pattern (constant-intensity in this case). A possible next step in this context is to generalize CI scattering states to more than one dimension. It is currently still an open question, however, whether this is possible at all or under which constraints this can work. A second direction that we are currently pursuing is to use our design principle not only to create waves with a constant intensity, but rather with any desired intensity profile inside a given medium [66, 67]. In preliminary calculations we find, e.g., that it is readily possible to create states that have a pronounced focus deep inside a disordered medium – a property that is very desirable for various applications in biophotonics and imaging. Last, but not least, we have also recently found [68] that a medium that supports CI scattering states can be made unidirectionally invisible. In this way we uncover a general design principle for unidirectional invisibility that goes far beyond the periodic structure with PT-symmetry discussed so far [11]. At this point we have to emphasize that these types of phenomena are based on complex wave interference and are therefore expected to exist in various areas of wave physics (optics, microwaves, acoustics, etc). As far as the experimental demonstration of such CI-waves is concerned, we have recently observed perfect transmission of acoustic CI-waves in disordered media [69]. These findings demonstrate that CI-waves have considerable potential for new exciting applications.

Acknowledgements This project was supported by the People Programme (Marie Curie Actions) of the European Union's Seventh Framework Programme (FP7/2007-2013) under REA Grant Agreement No. PIOFGA-2011-303228 (Project NOLACOME). K.G.M. is also supported by the European Union Seventh Framework Programme (FP7-REGPOT-2012-2013-1) under grant agreement 316165. S.R. acknowledges financial support by the Austrian Science Fund (FWF) through Project SFB NextLite (F49-P10) and Project GePartWave (I1142).

References

1. Leonhardt, U.: Optical conformal mapping. Science **312**, 1777–1780 (2006)
2. Tyson, R.K.: Principles of Adaptive Optics, 3rd edn. CRC Press, Boca Raton, London/New York (2001)
3. El-Ganainy, R., Makris, K.G., Khajavikhan, M., Musslimani, Z.H., Rotter, S., Christodoulides, D.N.: Non-Hermitian physics and PT symmetry. Nat. Phys. **14**, 11 (2018)
4. Moiseyev, N.: Non-Hermitian Quantum Mechanics. Cambridge University Press, Cambridge (2011)
5. Bender, C.M.: Making sense of non-Hermitian Hamiltonians. Rep. Prog. Phys. **70**, 947–1018 (2007)
6. Guo, A., Salamo, G.J., Duchesne, D., Morandotti, R., Volatier-Ravat, M., Aimez, V., Siviloglou, G.A., Christodoulides, D.N.: Observation of PT-symmetry breaking in complex optical potentials. Phys. Rev. Lett. **103**, 093902 (2009)
7. Rüter, C.E., Makris, K.G., El-Ganainy, R., Christodoulides, D.N., Segev, M., Kip, D.: Observation of parity–time symmetry in optics. Nat. Phys. **6**, 192–195 (2010)
8. Regensburger, A., Bersch, C., Miri, M.-A., Onishchukov, G., Christodoulides, D.N., Peschel, U.: Parity-time synthetic photonic lattices. Nature **488**, 167–171 (2012)
9. Feng, L., Xu, Y.-L., Fegadolli, W.S., Lu, M.-H., Oliveira, J.E.B., Almeida, V.R.,Chen, Y.-F., Scherer, A.: Experimental demonstration of a unidirectional reflectionless parity-time metamaterial at optical frequencies. Nat. Mater. **12**, 108–113 (2013)
10. Peng, B., Özdemir, Ş.K., Lei, F., Monifi, F., Gianfreda, M., Long, G.L., Fan, S., Nori, F., Bender, C.M., Yang, L.: Parity-time-symmetric whispering-gallery microcavities. Nat. Phys. **10**, 394–398 (2014)
11. Lin, Z., Ramezani, H., Eichelkraut, T., Kottos, T., Cao, H., Christodoulides, D.N.: Unidirectional invisibility induced by PT-symmetric periodic structures. Phys. Rev. Lett. **106**, 093902 (2011)
12. Chong, Y.D., Ge, L., Cao, H., Stone, A.D.: Coherent perfect absorbers: time-reversed lasers. Phys. Rev. Lett. **105**, 053901 (2010)
13. Wan, W., Chong, Y., Ge, L., Noh, H., Stone, A.D., Cao, H.: Time-reversed lasing and interferometric control of absorption. Science **331**, 889–892 (2011)
14. Sun, Y., Tan, W., H.-Q. Li, Li, J., Chen, H.: Experimental demonstration of a coherent perfect absorber with PT phase transition. Phys. Rev. Lett. **112**(14), 143903 (2014)
15. Liertzer, M., Ge, L., Cerjan, A., Stone, A.D., Türeci, H.E., Rotter, S.: Pump-induced exceptional points in lasers. Phys. Rev. Lett. **108**, 173901 (2012)
16. Brandstetter, M., Liertzer, M., Deutsch, C., Klang, P., Schöberl, J., Türeci, H.E., Strasser, G., Unterrainer, K., Rotter, S.: Reversing the pump dependence of a laser at an exceptional point. Nat. Commun. **5**, 4034 (2014)
17. Peng, B., Özdemir, Ş.K., Rotter, S., Yilmaz, H., Liertzer, M., Monifi, F., Bender, C.M., Nori, F., Yang, L.: Loss-induced suppression and revival of lasing. Science **346**, 328–332 (2014)
18. Bender, C.M., Brody, D.C., Jones, H.F.: Complex extension of quantum mechanics. Phys. Rev. Lett. **89**, 270401 (2002)
19. Makris, K.G., El-Ganainy, R., Christodoulides, D.N., Musslimani, Z.H.: Beam dynamics in PT symmetric optical lattices. Phys. Rev. Lett. **100**, 103904 (2008)
20. Musslimani, Z.H., Makris, K.G., El-Ganainy, R., Christodoulides, D.N.: Optical solitons in PT periodic potentials. Phys. Rev. Lett. **100**, 030402 (2008)
21. Chong, Y.D., Ge, L., Stone, A.D.: PT -symmetry breaking and laser-absorber modes in optical scattering systems. Phys. Rev. Lett. **106**, 093902 (2011)
22. Kottos, T.: Optical physics: broken symmetry makes light work. Nat. Phys. **6**, 166–167 (2010)
23. Makris, K.G., Ge, L., Türeci, H.E.: Anomalous transient amplification of waves in non-normal photonic media. Phys. Rev. X **4**, 041044 (2014)
24. Ambichl, P., Makris, K.G., Ge, L., Chong, Y., Stone, A.D., Rotter, S.: Breaking of PT-symmetry in bounded and unbounded scattering systems. Phys. Rev. X **3**, 041030 (2013)

25. Makris, K.G., Musslimani, Z.H., Christodoulides, D.N., Rotter, S.: Constant-intensity waves and their modulation instability in non-Hermitian potentials. Nat. Commun. **6**, 8257 (2015)
26. Makris, K.G., Musslimani, Z.H., Christodoulides, D.N., Rotter, S.: Constant intensity supermodes in non-Hermitian lattices. IEEE J. Sel. Top. Quantum Electron. **22**, 42–47 (2016)
27. Cole, J., Makris, K., Musslimani, Z., Christodoulides, D., Rotter, S.: Modulational instability in a PT-symmetric vector nonlinear Schrödinger system. Physica D Nonlinear Phenom. **336**, 53–61 (2016)
28. Makris, K.G., Brandstötter, A., Ambichl, P., Musslimani, Z.H., Rotter, S.: Wave propagation through disordered media without backscattering and intensity variations. Light Sci. Appl. **6**, e17030 (2017)
29. Durnin, J., Miceli, J.J., Eberly, J.H.: Diffraction-free beams. Phys. Rev. Lett. **58**, 1499–1501 (1987)
30. Tai, K., Hasegawa, A., Tomita, A.: Observation of modulational instability in optical fibers. Phys. Rev. Lett. **56**, 135–138 (1986)
31. Malendevich, R., Jankovic, L., Stegeman, G., Aitchison, J.S.: Spatial modulation instability in a Kerr slab waveguide. Opt. Lett. **26**, 1879 (2001)
32. Kip, D.: Modulation instability and pattern formation in spatially incoherent light beams. Science **290**, 495–498 (2000)
33. Meier, J., Stegeman, G.I., Christodoulides, D.N., Silberberg, Y., Morandotti, R., Yang, H., Salamo, G., Sorel, M., Aitchison, J.S.: Experimental observation of discrete modulational instability. Phys. Rev. Lett. **92**, 163902 (2004)
34. Lumer, Y., Plotnik, Y., Rechtsman, M.C., Segev, M.: Nonlinearly induced PT transition in photonic systems. Phys. Rev. Lett. **111**, 263901 (2013)
35. Zakharov, V.E., Gelash, A.A.: Nonlinear stage of modulation instability. Phys. Rev. Lett. **111**, 054101 (2013)
36. Schwartz, T., Bartal, G., Fishman, S., Segev, M.: Transport and Anderson localization in disordered two-dimensional photonic lattices. Nature **446**, 52–55 (2007)
37. Lahini, Y., Avidan, A., Pozzi, F., Sorel, M., Morandotti, R., Christodoulides, D.N., Silberberg, Y.: Anderson localization and nonlinearity in one-dimensional disordered photonic lattices. Phys. Rev. Lett. **100**, 013906 (2008)
38. Billy, J., Josse, V., Zuo, Z., Bernard, A., Hambrecht, B., Lugan, P., Clément, D., Sanchez-Palencia, L., Bouyer, P., Aspect, A.: Direct observation of Anderson localization of matter waves in a controlled disorder. Nature **453**, 891–894 (2008)
39. Lagendijk, A., Tiggelen, B.V., Wiersma, D.S.: Fifty years of Anderson localization. Phys. Today **62**, 24–29 (2009)
40. Segev, M., Silberberg, Y., Christodoulides, D.N.: Anderson localization of light. Nat. Photonics **7**, 197–204 (2013)
41. Basiri, A., Bromberg, Y., Yamilov, A., Cao, H., Kottos, T.: Light localization induced by a random imaginary refractive index. Phys. Rev. A **90**, 043815 (2014)
42. Lagendijk, A., van Tiggelen, B.A.: Resonant multiple scattering of light. Phys. Rep. **270**, 143–215 (1996)
43. Akkermans, E., Montambaux, G.: Mesoscopic Physics of Electrons and Photons. Cambridge University Press, Cambridge (2007)
44. Sebbah, P.: Waves and Imaging Through Complex Media. Springer, Netherlands/Dordrecht (2001) OCLC: 863932944
45. Beenakker, C.W.J.: Random-matrix theory of quantum transport. Rev. Mod. Phys. **69**, 731–808 (1997)
46. Mosk, A.P., Lagendijk, A., Lerosey, G., Fink, M.: Controlling waves in space and time for imaging and focusing in complex media. Nat. Photonics **6**, 283–292 (2012)
47. Rotter, S., Gigan, S.: Light fields in complex media: mesoscopic scattering meets wave control. Rev. Mod. Phys. **89**, 015005 (2017)
48. Vellekoop, I.M., Mosk, A.P.: Focusing coherent light through opaque strongly scattering media. Opt. Lett. **32**, 2309 (2007)

49. Popoff, S.M., Lerosey, G., Carminati, R., Fink, M., Boccara, A.C., Gigan, S.: Measuring the transmission matrix in optics: an approach to the study and control of light propagation in disordered media. Phys. Rev. Lett. **104**, 100601 (2010)
50. Vellekoop, I.M., Lagendijk, A., Mosk, A.P.: Exploiting disorder for perfect focusing. Nat. Photonics **4**, 320–322 (2010)
51. Katz, O., Small, E., Bromberg, Y., Silberberg, Y.: Focusing and compression of ultrashort pulses through scattering media. Nat. Photonics **5**, 372–377 (2011)
52. McCabe, D.J., Tajalli, A., Austin, D.R., Bondareff, P., Walmsley, I.A., Gigan, S., Chatel, B.: Spatio-temporal focusing of an ultrafast pulse through a multiply scattering medium. Nat. Commun. **2**, 447 (2011)
53. Yaqoob, Z., Psaltis, D., Feld, M.S., Yang, C.: optical phase conjugation for turbidity suppression in biological samples. Nat. Photonics **2**, 110–115 (2008)
54. Riboli, F., Caselli, N., Vignolini, S., Intonti, F., Vynck, K., Barthelemy, P., Gerardino, A., Balet, L., Li, L.H., Fiore, A., Gurioli, M., Wiersma, D.S.: Engineering of light confinement in strongly scattering disordered media. Nat. Mater. **13**, 720–725 (2014)
55. Bruck, R., Vynck, K., Lalanne, P., Mills, B., Thomson, D.J., Mashanovich, G.Z., Reed, G.T., Muskens, O.L.: All-optical spatial light modulator for reconfigurable silicon photonic circuits. Optica **3**, 396 (2016)
56. Bachelard, N., Gigan, S., Noblin, X., Sebbah, P.: Adaptive pumping for spectral control of random lasers. Nat. Phys. **10**, 426–431 (2014)
57. Hisch, T., Liertzer, M., Pogany, D., Mintert, F., Rotter, S.: Pump-controlled directional light emission from random lasers. Phys. Rev. Lett. **111**, 023902 (2013)
58. Schönhuber, S., Brandstetter, M., Hisch, T., Deutsch, C., Krall, M., Detz, H., Andrews, A.M., Strasser, G., Rotter, S., Unterrainer, K.: Random lasers for broadband directional emission. Optica **3**, 1035 (2016)
59. Ge, L., Malik, O., Türeci, H.E.: Enhancement of laser power-efficiency by control of spatial hole burning interactions. Nat. Photonics **8**, 871–875 (2014)
60. Liew, S.F., Redding, B., Ge, L., Solomon, G.S., Cao, H.: Active control of emission directionality of semiconductor microdisk lasers. Appl. Phys. Lett. **104**, 231108 (2014)
61. Bender, C.M., Orszag, S.A.: Advanced Mathematical Methods for Scientists and Engineers. 1: Asymptotic Methods and Perturbation Theory. Springer, New York (2009). OCLC: 837310111
62. Yeh, P.: Optical Waves in Layered Media. Wiley-Interscience, Hoboken (2005)
63. Wang, J., Genack, A.Z.: Transport through modes in random media. Nature **471**, 345–348 (2011)
64. Peña, A., Girschik, A., Libisch, F., Rotter, S., Chabanov, A.A.: The single-channel regime of transport through random media. Nat. Commun. **5**, 3488 (2014)
65. Szameit, A., Nolte, S.: Discrete optics in femtosecond-laser-written photonic structures. J. Phys. B Atomic Mol. Phys. **43**(16), 163001 (2010)
66. Brandstötter, A., Makris, K.G., Rotter, S.: Non-Hermitian focusing deep inside strongly disordered scattering media. In: IEEE, CLEO Europe, European Quantum Electronics Conference, EJ_P_1, June 2017, pp. 1–1
67. Makris, K.G., Brandstötter, A., Rotter, S.: Wave control in non-Hermitian disordered media. IEEE, Photonics Conference (IPC), Oct. 2017, pp. 391–392
68. Brandstötter, A., Makris, K., Rotter, S.: Non-Hermitian invisibility based on constant-intensity waves, p. FM4B.4. Frontiers in Optics, OSA (2017)
69. Rivet, E., Brandstötter, A., Makris, K. G., Lissek, H., Rotter, S., Fleury, R.: Constant-pressure sound waves in non-Hermitian disordered media. Nat. Phys. Published online at https://doi.org/10.1038/s41567-018-0188-7